Optimizing Biosensing Properties on Undecylenic Acid-Functionalized Diamond

Yu Lin Zhong,[†] Kwok Feng Chong,[†] Paul W. May,[§] Zhi-Kuan Chen,[‡] and Kian Ping Loh*,[†]

Department of Chemistry, National University of Singapore, 3 Science Drive 3, Singapore 117543, Institute of Materials Research and Engineering, 3 Research Link, Singapore 117602, and School of Chemistry, University of Bristol, Bristol BS8 1TS, UK

Received December 18, 2006. In Final Form: February 8, 2007

The optimization of biosensing efficiency on a diamond platform depends on the successful coupling of biomolecules on the surface, and also on effective signal transduction in the biorecognition events. In terms of biofunctionalization of diamond surfaces, surface electrochemical studies of diamond modified with undecylenic acid (UA), with and without headgroup protection, were performed. The direct photochemical coupling method employing UA was found to impart a higher density of carboxylic acid groups on the diamond surface compared to that using trifluoroethyl undecenoate (TFEU) as the protecting group during the coupling process. Non-faradic impedimetric DNA sensing revealed that lightly doped diamond gives better signal transduction sensitivity compared to highly doped diamond.

1. Introduction

Boron-doped diamond (BDD) exhibits various desirable properties such as biocompatibility,[1] excellent thermal conductivity, high charge carrier mobility, large electrochemical potential window, chemical inertness, and hardness, making it suitable for application in electronic devices,[2] biosensing[3,4] and cell cultures.[5,6] Recent breakthroughs in the synthesis of nanocrystalline diamond (NCD) using chemical vapor deposition (CVD) opens up tremendous possibilities in surface coatings,[7] and also integration with conventional microelectronic processing. An as-grown diamond film is terminated by hydrogen on the surface and is chemically inert and hydrophobic. This creates problems for the attachment of many biomolecules which are inherently hydrophilic. Therefore, the diamond surface has to be modified with biocompatible functional groups such as carboxylic acids, amines, or alcohols for subsequent attachment to biomolecules. Several approaches for functionalizing diamond have been reported; these include photochemical grafting of molecules bearing terminal vinyl group,[8,9] electrochemical reduction of aryldiazonium salts,[10,11] electropolymerization of conduction polymers,[12] halogenation of diamond surfaces with subsequent organic functionalization,[13] wet-chemical modification with alkanoic acid initiated by organic peroxide,[14] and introduction of oxygen-containing functional groups by oxygen plasma.[15] In the area of microelectronic processing, the photochemical functionalization method is preferred over wet-chemical modification as it allows facile patterning of the platform with functional groups. It has been suggested that photochemical functionalization is a surface-mediated photochemical reaction initiated by the photoejection of electrons from the H-terminated, negative electron affinity diamond to the monomer liquid phase.[16]

In this work, we immobilized probe DNA on a diamond platform via UV-photochemical functionalization of alkene acid-type molecules, e.g., undecylenic acids (UA). Because UA is a bifunctional molecule, a priori it is not known which functional group at the ends will react preferentially with diamond under UV photochemical activation. For example, the photochemical coupling method developed by Hamers and co-workers on silicon,[17] and later adapted for diamond,[8] requires the protection of the headgroups (carboxylic or amine end) during the coupling process, to ensure that photochemical coupling with unsaturated bonds occurs as desired; otherwise, reaction with the amine headgroups may cause etching of the substrate, as has been observed previously for silicon surfaces.[18] However, it is also possible that the highly inert nature of diamond precludes reaction with these headgroups. It is certainly beneficial to identify a convenient way of coupling carboxylic functionalities on the diamond surface without tedious protection and deprotection steps, and this provides the motivation for this work. Other

* Corresponding author. E-mail: chmlohkp@nus.edu.sg.
† National University of Singapore.
‡ Institute of Materials Research and Engineering.
§ University of Bristol.

(1) Garguilo, J. M.; Davis, B. A.; Buddie, M.; Kock, F. A. M.; Nemanich, R. J. *Diamond Relat. Mater.* **2004**, *13*, 595.
(2) Kohn, E.; Adamschik, M.; Schmid, P.; Ertl, S.; Floter, A. *Diamond Relat. Mater.* **2001**, *10*, 1684.
(3) Poh, W. C.; Loh, K. P. *Langmuir* **2004**, *20*, 5484.
(4) Christiaens, P.; Vermeeren, V.; Wenmackers, S.; Daenen, M.; Haenen, K.; Nesládek, M.; vandeVen, M.; Ameloot, M.; Michiels, L.; Wagner, P. *Biosens. Bioelectron.* **2006**, *22*, 170.
(5) Huang, T. S.; Tzeng, Y.; Liu, Y. K.; Chen, Y. C.; Walker, K. R.; Guntupalli, R.; Liu, C. *Diamond Relat. Mater.* **2004**, *13*, 1098.
(6) Ariano, P.; Baldelli, P.; Carbone, E.; Vittone, E. *Diamond Relat. Mater.* **2005**, *14*, 669.
(7) Gowri, M.; Li, H.; Kacsich, T.; Schermer, J. J.; van Enckevort, W. J. P.; ter Meulen, J. J. *Surf. Coat. Technol.* **2007**, *201*, 460.
(8) Yang, W.; Auciello, O.; Bulter, J. E.; Cai, W.; Carlisle, J. A.; Gerbi, J. E.; Gruden, D. M.; Knickerbocker, T.; Lasseter, T. L.; Russell, J. N., Jr.; Smith, L. M.; Hamers, R. J. *Nat. Mater.* **2002**, *1*, 253.
(9) Nebel, C. E.; Shin, D.; Takeuchi, D.; Yamamoto, T.; Watanabe, H.; Nakamura T. *Langmuir* **2006**, *22*, 5645.
(10) Wang, J.; Firestone, M. A.; Auciello, O.; Carlisle, J. A. *Langmuir* **2004**, *20*, 11450.
(11) Shin, D.; Rezek1, B.; Tokuda1, N.; Takeuchi, D.; Watanabe, H.; Nakamura, T.; Yamamoto, T.; Nebel, C. E. *Phys. Status Solidi (a)* **2006**, *203*, 3245.
(12) Gu, H.; Su, X. D.; Loh, K. P. *J. Phys. Chem. B* **2005**, *109*, 13611.
(13) Liu, Y.; Gu, Z. N.; Margrave, J. L.; Khabashesku, V. N. *Chem. Mater.* **2004**, *16*, 3924.
(14) Tsubota, T.; Tanii, S.; Ida, S.; Nagata, M.; Matsumoto, Y. *Phys. Chem. Chem. Phys.* **2003**, *5*, 1474.
(15) Notsu, H.; Yagi, I.; Tatsuma, T.; Tryk, D. A.; Fujishima, A. *Electrochem. Solid State Lett.* **1999**, *2*, 522.
(16) Nichols, B. M.; Butler, J. E.; Russell, J. N.; Hamers, R. J. *J. Phys. Chem. B* **2005**, *109*, 20938.
(17) Strother, T.; Cai, W.; Zhao, X.; Hamers, R. J.; Smith, L. M. *J. Am. Chem. Soc.* **2000**, *122*, 1205.
(18) Strother, T.; Knickerbocker, T.; Russell, J. N., Jr.; Butler, J. E.; Smith, L. M.; Hamers, R. J. *Langmuir* **2002**, *18*, 968.

10.1021/la063658k CCC: $37.00
Published on Web 04/10/2007

Scheme 1. Reaction Sequences Illustrating the Conversion of UA to TFEU and the Subsequent Deprotection of TFEU To Allow Coupling to DNA via EDC/NHS Carbodiimide Chemistry

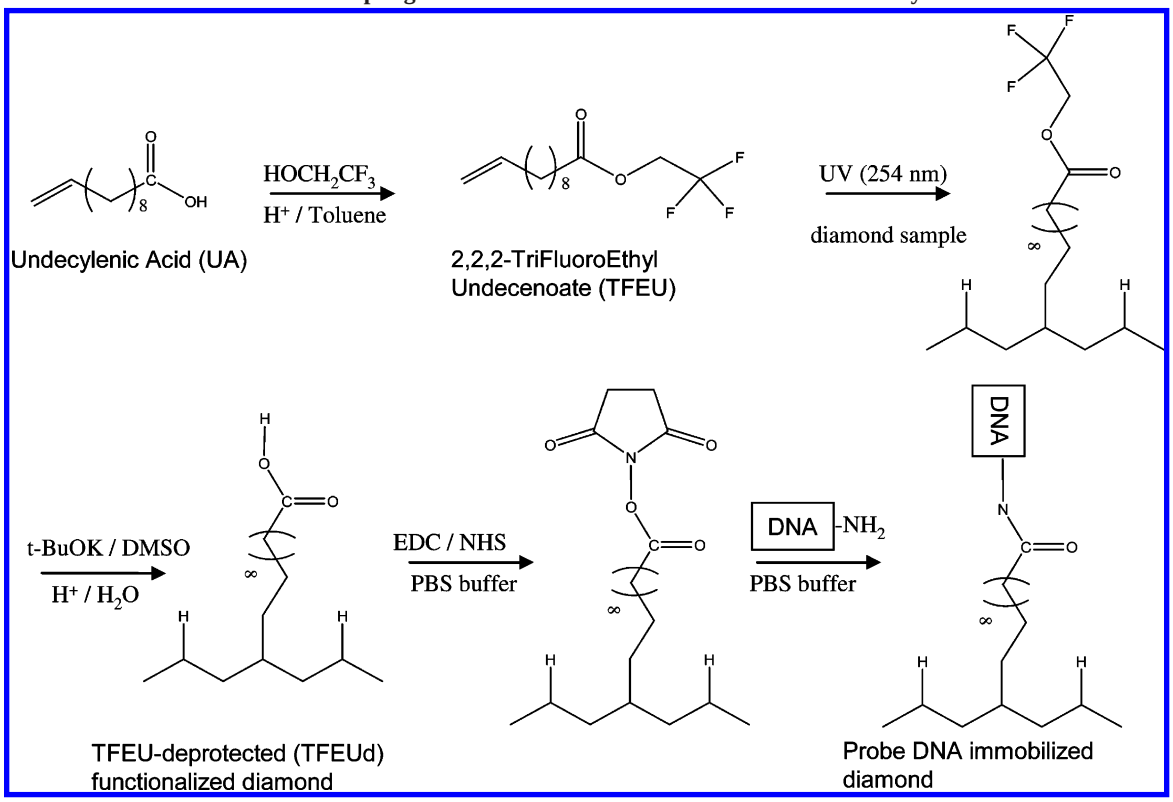

important factors for imparting efficient signal transduction property on the diamond platform were also investigated in this study.

2. Experimental Section

Chemical Reagents. All reagent grade chemicals were purchased and used as received from Sigma-Aldrich unless otherwise stated. Na_3PO_4 buffer (0.1 M, pH 7.0) was purchased from 1st Base. All 30 bases oligonucleotides were synthesized by MWG Biotech. The probe DNA is modified at the 5′ end with an alkylamino modifier ($NH_2-C_{12}-$5′-GCA CCT GAC TCC TGT GGA GAA GTC TGC CGT-3′) for immobilization. The target DNA contains a fully complementary sequence for impedimetric sensing (5′-ACG GCA GAC TTC TCC ACA GGA GTC AGG TGC-3′). The complementary target for patterned DNA was fluorescein labeled (FAM) at the 5′ end. All dilution and preparation of redox electrolytes for electrochemical work were made with Nanopure water (18.0 MΩ cm).

Preparation of Diamond Substrates. Fifty micrometer thick sub-microcrystalline diamond (sMCD) films were grown on *p*-type Si substrates in a commercial 2.45 GHz microwave plasma reactor (Astex) using methanol and boron oxide mixtures according to an established procedure.[19] The diamond sample had a surface resistance of 10 Ω cm and the boron doping level was approximately 10^{19} cm^{-3}. These sMCD samples were used throughout the experiments unless otherwise stated. For investigation of the boron dopant effect, microcrystalline diamond (MCD) films were grown in a hot filament reactor (with 2 sccm CH_4, 200 sccm H_2, and 0.5 sccm of B_2H_6 of varying concentrations: 0.1, 4.4, and 22.8 ppm with respect to H_2; conditions: 20 Torr for 7 h).

Acid cleaning and hydrogen plasma cleaning of diamond were used for all diamond samples. Metallic impurities were first dissolved in hot aqua regia (HNO_3:HCl = 1:3), followed by removal of organic impurities from the diamond samples by hot "piranha" solution (H_2O_2:H_2SO_4 = 1:3) at 90 °C. Microwave hydrogen plasma treatment was performed using 800 W microwave power and 300 sccm of hydrogen gas flow for 15 min.

Synthesis of TFEU. The general biofunctionalization process of diamond samples is depicted in Scheme 1. The synthesis and UV photochemical grafting of 2,2,2-trifluoroethyl undecenoate (TFEU) was performed following reported procedures.[17,18] In brief, TFEU was synthesized by esterification of undecylenic acid (UA) and 2,2,2-trifluoroethanol with a catalytic amount of sulfuric acid in toluene. After extraction and typical workup, the crude product was purified by vacuum distillation followed by column chromatography purification and its identity was confirmed by proton and carbon NMR.

UV Photochemical Functionalization. In a homemade stainless steel vacuum chamber with constant nitrogen purging, the H-terminated diamond samples were covered with a thin layer of monomer and exposed to UV light (254 nm; 18 W) through a quartz window for 18 h. To achieve patterned functionalized surfaces, copper TEM grids (SPI) of various mesh numbers were aligned on the diamond surfaces prior to covering with monomer. After UV exposure, all samples were rinsed three times in 10% SDS solution, Nanopure water, THF, and hexane. For UA-functionalized samples, additional rinsing in hot acetic acid was done to remove the hydrogen-bonded UA layer.[20] For TFEU-functionalized samples, hydrolysis was performed by dipping the samples in 250 mM solution of potassium *tert*-butoxide in DMSO for 3 min at room temperature followed by rinsing in acidified water to obtain a TFEUd (TFEU-deprotected) functionalized diamond sample.

Surface Characterization. X-ray photoelectron spectroscopy (XPS) was performed with a VG ESCALAB MkII spectrometer using an unmonochromated Mg Kα X-ray source (1253.6 eV). The pass energy of the hemisphere analyzer was maintained at 50 eV for a wide scan and 20 eV for a narrow scan, while the takeoff angle was fixed at 15° with respect to sample normal. Static secondary ion mass spectrometry (SSIMS) was carried out in a TOF-SIMS IV

(19) Rao, T. N.; Yagi, I.; Miwa, T.; Tryk, D. A.; Fujishima, A. *Anal. Chem.* **1999**, *71*, 2506.

(20) Faucheux, A.; Gouget-Laemmel, A. C.; Henry de Villeneuve, C.; Boukherroub, R.; Ozanam, F.; Allongue, P.; Chazaviel, J.-N. *Langmuir* **2006**, *22*, 153.

instrument using a low ion dose of less than 10^{-12} ions/cm^2. It was equipped with a time-of-flight ion mass analyzer with a mass resolution above 7000. The ion beam source used was Ga ion with a beam energy of 25 keV and a pulse width of 25 ns. All the spectra obtained were normalized against their total counts from *m*/*z* of 2 to *m*/*z* of 200.

Contact Angle and COOH Density Determination. A drop (3 μL) of pure water was placed on the sample surface to form a sessile drop in which the contact angle was measured by a Rame-Hart Contact Angle Goniometer. On each sample surface, the experiment was carried out three times and the average contact angle value was obtained. The surface carboxylic acid group density was quantified using the Toluidine Blue O (TBO) method.[21] In brief, functionalized diamond samples (1 cm^2) were soaked in 5×10^{-4} M TBO solution and adjusted to pH 10 with NaOH. Formation of ionic complexes between the surface carboxylic acid groups and the cationic dye was allowed to proceed for 5 h at room temperature, followed by rinsing of the samples with NaOH solution to remove the uncomplexed TBO molecules. Desorption of the dye was performed in 50 wt % acetic acid solution and its amount was calculated from its optical density at 633 nm, using a calibrated plot. For each type of functionalized diamond, four samples were evaluated and the average reading was taken.

DNA Immobilization and Target Hybridization. For immobilization of the probe DNA, the functionalized diamond samples were first immersed in a 1:1 mixture (in 0.1 M Na_3PO_4 buffer solution) of 400 mM EDC and 100 mM NHS for 1 h to activate the carboxylic acid group through the formation of an NHS-ester intermediate. After being rinsed with buffer solution, the samples were covered with 20 μM probe DNA (in 0.1 M Na_3PO_4 buffer solution) and left overnight for incubation in a humidity-controlled container, before the unreacted carboxylic acid groups were finally saturated with 0.1 M ethanolamine solution for 1 h. For hybridization of the target DNA, the biofunctionalized diamond samples were covered with 20 μM target DNA in hybridization buffer (2× SSC buffer solution, pH 7.0, containing 0.3 M NaCl and 0.03 M sodium citrate). For denaturing, the hybridized samples were soaked in 0.1 M NaOH solution for 30 min at room temperature and followed by copious rinsing with buffer solution. After each treatment step involving DNA, the samples were soaked and rinsed in washing buffer (0.2% SDS in PBS buffer) for at least 15 min to ensure that the surface is free of physisorbed DNA. For patterned DNA samples, the fluorescein (FAM) labeled complementary DNA targets were assayed by a fluorescence microscope (Olympus BX60).

Electrochemical System. All electrochemical measurements were carried out in a single-compartment Teflon cell with a three-electrode configuration system: a diamond working electrode, Ag/AgCl reference electrode (3.0 M KCl), and a Pt mesh counter electrode. For all electrochemical experiments, a small area (0.07 cm^2) of the diamond surface was exposed to the electrolyte through a Viton O-ring, unless otherwise stated. Top contact on the diamond sample surface was made through an Au-plated probe. Electrochemical impedance spectroscopy (EIS) was carried out using a potentiostat/galvanostat unit equipped with a frequency response analyzer module (Autolab/PGSTAT30, Eco Chemie B.V.) and data analysis was performed using the frequency response analyzer (FRA).

All impedance spectra were collected from 10 kHz to 0.1 Hz, at an ac amplitude of 10 mV and performed at open circuit potential (OCP), unless otherwise stated. Single strength phosphate buffer solution (PBS) was used as the electrolyte throughout most electrochemical measurements. For pH-dependent experiments, Fe-redox electrolytes were prepared from 5 mM $K_2Fe(CN)_6$ and 5 mM $K_3Fe(CN)_6$ in 0.1 M KCl, and these were acidified or basified as required by 0.1 M HCl or 0.1 M KOH, respectively.

3. Results and Discussion

Surface Science Characterization. Figure 1 shows the XPS wide scan for all samples. Only elements of corresponding

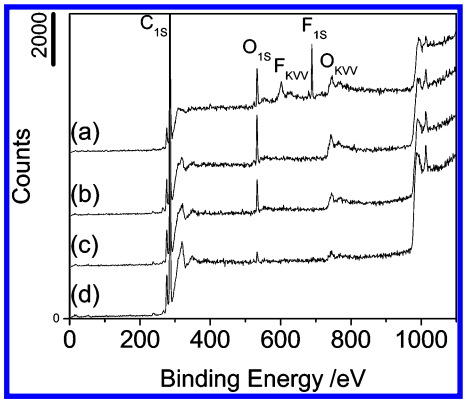

Figure 1. XPS wide scan spectrum of (a) TFEU-functionalized, (b) TFEU-deprotected (TFEUd) functionalized, (c) UA-functionalized, and (d) cleaned H-terminated diamond.

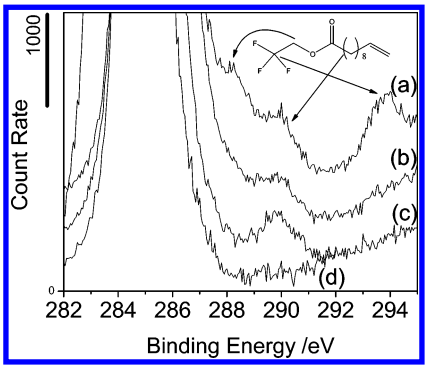

Figure 2. XPS C_{1s} narrow scan of (a) TFEU-functionalized, (b) TFEU-deprotected (TFEUd) functionalized, (c) UA-functionalized, and (d) cleaned H-terminated diamond.

functional groups are present without any other impurity. The success of TFEU deprotection is evident with the complete disappearance of F_{1s} (698 eV) and F_{KVV} peaks. The diamond samples were recycled for experiments by cleaning with hydrogen plasma, and spectrum 1d shows the XPS wide scan of a cleaned H-terminated diamond having only a trace amount of oxygen/oxides (533 eV). The XPS C_{1s} narrow scans, shown in Figure 2, proved the presence of the expected functional groups from the chemically shifted peaks. The intense bulk carbon peaks at 284.5 eV were not shown in Figure 2 to highlight the chemically shifted peaks. The chemically shifted peaks at 289.8, 293.7, and 288.0 eV for TFEU-functionalized diamond sample are attributed to the photoionization of carbon atoms originating from the carbonyl group (COO), the CF_3 group, and the CCF_3 group, respectively. Similar to previously reported results, deprotection resulted in the loss of CF_3CH_2OH; subsequently, only the peak due to the COOH group (289.8 eV) remained.[18] In a comparison of the TFEUd (deprotected TFEU) and UA-functionalized diamond sample, the latter shows a more intense carboxylic-related C_{1s} peak at 289.9 eV. An explanation is that the strong base used in the deprotection of TFEU resulted in damage of the monolayer and reduced its coverage.[22]

The positive ion TOF-SIMS spectra of functionalized diamond (not shown) contain peaks of hydrocarbon fragments which originated from the organic monolayer and bulk diamond. To characterize the surface functionalities of electronegative elements, the negative ion TOF-SIMS spectra were recorded. From Figure 3, the negative TOF-SIMS spectra of functionalized diamond show prominent characteristic peaks associated with alkyl COOH found at *m*/*z* 41 ($CHCO^-$), 45 ($CH_3CH_2O^-$), 58

(21) Uchida, E.; Uyama, Y.; Ikada, Y. *Langmuir* **1993**, *9*, 1121.

(22) Liu, Y.-J.; Navasero, N. M.; Yu, H.-Z. *Langmuir* **2004**, *20*, 4039.

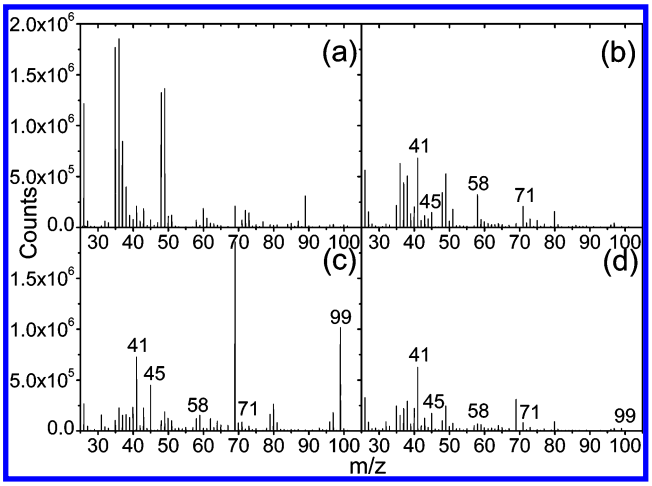

Figure 3. Negative ion TOF-SIMS spectrum of (a) H-terminated, (b) UA-functionalized, (c) TFEU-functionalized, and (d) TFEU-deprotected (TFEUd) functionalized diamond.

Table 1. Contact Angles and COOH Densities of Various Diamond Samples

diamond sample	water contact angle (deg)	COOH density (molecules cm^{-2})
H-terminated	90.9 (±1.0)	
TFEU	101.0 (±1.1)	
TFEUd	85.3 (±2.0)	$1.6\ (\pm0.4) \times 10^{14}$
UA	75.0 (±0.8)	$4.8\ (\pm0.5) \times 10^{14}$

($CH_2{=}COO^-$), 59 ($C_3H_7O^-$, CH_3COO^-), and 71 ($CH_2{=}CHCOO^-$), these peaks are insignificant in the spectrum of H-terminated diamond. The deprotection step of TFEU was judged to be successful, as evidenced by the disappearance of the intense peak at *m*/*z* 99, attributed to the protecting/leaving group $CF_3CH_2O^-$. However, the deprotection step also caused an overall decrease in intensity of those characteristic peaks associated with the monolayer functionalities. As such, the intensity of those peaks are found to be stronger in UA-functionalized diamond compared to TFEUd-functionalized diamond, which suggests that the surface COOH coverage is higher for UA-functionalized diamond.

Contact Angle and COOH Density Determination. From Table 1, the functionalization process of diamond was easily monitored by contact angle goniometry which assesses the hydrophilicity of the sample surface. For TFEU-functionalized diamond, its surface first became more hydrophobic due to the CF_3 end groups, but its contact angle decreased upon deprotecting these groups. The COOH densities of functionalized diamond is on the order of 10^{14} cm^2, which is consistent with the formation of a dense monolayer.[8] As expected, the COOH densities of functionalized diamond complement well their contact angle measurements in which more hydrophilic COOH groups resulted in lower water contact angles. Our results show that UA-functionalized diamond is more hydrophilic due to its higher COOH density as determined by the TBO method.

pH-Dependent Electrochemical Characterization. In the 0.1 mM Fe-redox couple electrolyte, a Nyquist plot (not shown) of H-terminated diamond at open circuit potential (OCP), and at different pH values, show similar characteristics: a semicircle followed by a 45° straight line. This implies that the charge-transfer resistance (R_{CT}) across H-terminated diamond (highly doped) is small and limited only by Warburg diffusion at all pH. However, UA- and TFEUd-functionalized diamond show pronounced increase in charge-transfer resistance with increasing pH, as shown in Figure 4. This characteristic pH-dependent behavior is due to deprotonation of COOH groups at increasing

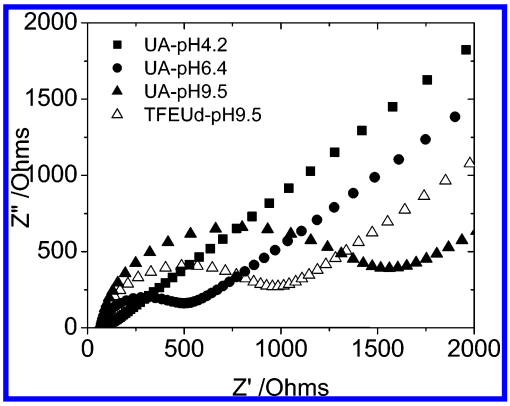

Figure 4. Nyquist plot of UA- and TFEUd-functionalized diamond in 0.1 mM Fe-redox couple electrolyte of different pH: 4.2 (■), 6.4 (●), and 9.5 (▲). (Note: only the Nyquist plot of TFEUd-functionalized diamond at pH 9.5 is shown for clarity. Electrode area = 0.2 cm^2.)

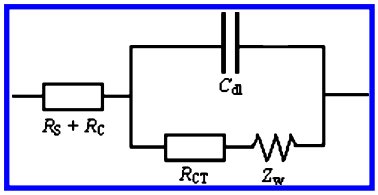

Figure 5. Equivalent circuit model which was used for (a) UA-functionalized diamond electrodes in 0.1 mM Fe-redox couple/0.1 M KCl electrolyte.

pH, which creates an anionic barrier against charge transfer of the negatively charged ferrocyanide ions. Results show that UA-functionalized diamond possesses consistently higher charge-transfer resistance than TFEUd-functionalized diamond at all pHs (although only the Nyquist plot of TFEUd-functionalized diamond at pH 9.5 is shown for clarity). Again, this indicates that UA-functionalized diamond has a higher carboxylic acid density than TFEUd, or forms a more complete passivating layer on the surface.

An estimate of the R_{CT} values in Figure 4 can be found by extrapolating the semicircle to intercept the Z' axis, but a more accurate value was obtained by fitting the impedance data to a simple Randles equivalent circuit with additional Warburg impedance as shown in Figure 5. The R_{CT} can be equated to the exchange current under equilibrium, I_o, from eq 1 where $R = 8.31\ J\ mol^{-1}\ K^{-1}$ is the gas constant, $T = 300$ K is the experimental temperature, $n = 1$ is the number of electrons transferred per molecule of the redox probe, and $F = 9.65 \times 10^4$ C $equiv^{-1}$ is the Faraday constant. The heterogeneous charge-transfer rate constant (k_{CT}) can be evaluated from eq 2, where $A = 0.2$ cm^2 is the area of exposed diamond electrode and $[S] = 1 \times 10^{-6}$ mol cm^{-3} is the bulk concentration of redox probe.

$$R_{CT} = RT(nFI_o)^{-1} \quad (1)$$

$$I_o = nFAk_{CT}[S] \quad (2)$$

Table 2 presents the R_{CT} values extracted from equivalent circuit modeling and their respective k_{CT} values. The heterogeneous charge-transfer rate constant of UA-functionalized diamond is slightly smaller than TFEUd-functionalized diamond under acidic conditions, but it is almost 2 orders of magnitude smaller under basic conditions. It can be inferred that the carboxylic functionalities of UA-functionalized diamond are outward-facing and active, and that a higher coverage of such exists on UA-functionalized diamond.

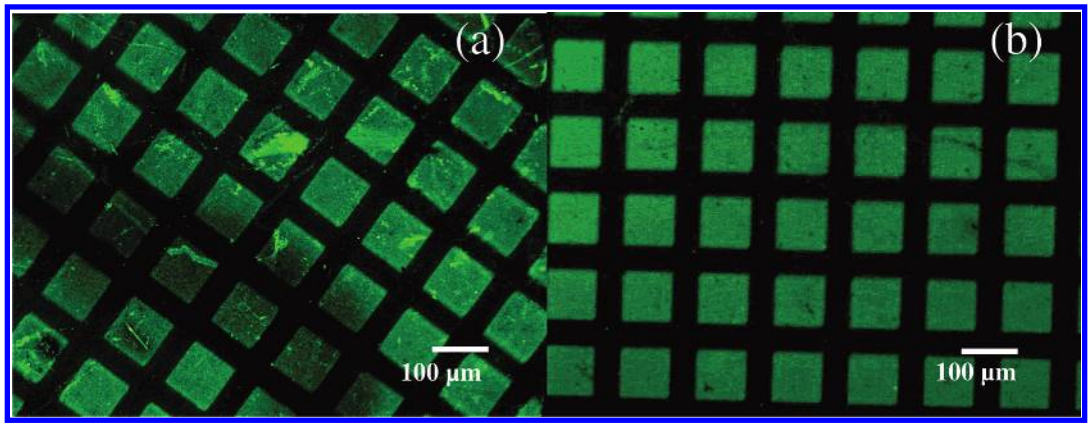

Figure 6. Patterned fluorescence images of FITC-labeled DNA immobilized on diamond which has been biofunctionalized with (a) UA and (b) TFEUd and subjected to repeated denature−rehybridization cycles (three cycles).

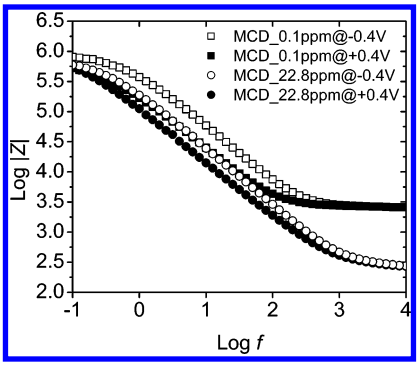

Figure 7. Bode plot (impedance (Z) vs frequency (f)) of UA-functionalized MCD_0.1 ppm (■) and MCD_22.8 ppm (●) at +0.4 V (shaded) and −0.4 V (open circles). The lightly doped diamond exhibits a larger dispersion of impedance as a function of applied voltage compared to the more heavily doped diamond.

Fluorescence Imaging of DNA Hybridization. To show that the UV photochemical functionalization method is amenable to lithographical patterning of biomolecules on the surface, copper TEM grids (Structure Probe, Inc.) were employed as a mask during UV light exposure to create patterned functionalized diamond surfaces. After probe DNA immobilization via EDC/NHS activation, well-defined and highly stable patterned DNA surfaces were achieved. Figure 6a and 6b show well-defined fluorescence images of labeled complimentary target DNA on diamond surfaces functionalized with UA and TFEU. These images were recorded after three denature−rehybridization cycles. Storage of the biofunctionalized diamond samples for weeks caused little decrease in the fluorescence intensity.

Effect of Boron Dopant Concentration. Three UA-functionalized MCD samples of different boron dopant concentration, namely, MCD_0.1 ppm, MCD_4.4 ppm, and MCD_22.8 ppm, were characterized by Mott−Schottky analysis in PBS. The dopant concentration, N_A, can be found by obtaining the gradient $(d(1/C^2)/dV)$ from a Mott−Schottky plot (not shown) according to eq 3, where C is the effective capacitance, V is the applied potential, e is the electron charge, ϵ_0 is the permittivity of free space, and ϵ is the dielectric constant of the semiconductor.

$$N_A = -(2/e\epsilon_0\epsilon)\,(d(1/C^2)/dV)^{-1} \quad (3)$$

The calculated boron dopant concentration for MCD_0.1 ppm, MCD_4.4 ppm, and MCD_22.8 ppm are 8.9×10^{17}, 8.1×10^{18}, and 1.8×10^{19} cm^{-1}, respectively, which correlate well with the level of boron gas used during their growth. Next, EIS was carried out on UA-functionalized MCD samples at different bias voltages (vs 3.0 M Ag/AgCl) and their impedance data (results of MCD_4.4 ppm not shown for clarity) are presented in a Bode plot, as shown in Figure 7. All the doped MCD samples showed p-type characteristics; i.e., their impedance value is lower at positive applied voltage due to accumulation of holes and higher at negative applied voltage due to carrier depletion. In our experimental setup, this voltage-dependent behavior owing to the diamond space-charge exists at frequencies between 1 Hz and 1 kHz for doped diamond. Above that, the impedance is limited by the solution and contact resistance, while below that, charge-transfer process sets in.

Impedance Response. The impedance response of the UA-functionalized diamond shows a profile that depends on the doping level of the diamond when we carried out faradic impedimetric study using a 0.1 mM ferrocyanide couple. Typically, the doped diamond which had been functionalized with UA displayed a single semicircular loop in the Nyquist plot (boron: 10^{18-19} cm^{-1}) as shown in Figure 8a, whereas two semicircular loops can be observed in nominally undoped, UA-functionalized diamond (boron < 10^{17} cm^{-1}) in Figure 8b. The two semicircular loops can be fitted to two RC time constants in equivalent circuit modeling. The lower frequency loop has remarkably strong pH-dependent behavior, which may be attributed to changes in charging capacitance and transfer resistance arising from the protonation/deprotonation of the UA molecular layer. At higher pH, a pronounced increase in the diameter of the low frequency loop can be observed in Figure 8b. For nominally undoped diamond, the difference in R_{CT} values at basic and acidic conditions is on the order of 700 kΩ, while for doped diamond, the difference is merely 8 kΩ. This suggests that changes in surface double-layer characteristics affect the charge-transfer resistance of the undoped diamond dramatically. One reason may be due to the influence of this double layer on the space

Table 2. R_{CT} and k_{CT} of UA-Functionalized and TFEUd-Functionalized Diamond at Various pH

diamond sample	pH 4.2		pH 6.4		pH 9.2	
	R_{CT} (Ω)	k_{CT} (cm s^{-1})	R_{CT} (Ω)	k_{CT} (cm s^{-1})	R_{CT} (Ω)	k_{CT} (cm s^{-1})
UA	43.4	3.08×10^{-2}	392	3.41×10^{-3}	1347	9.94×10^{-4}
TFEUd	25.1	5.33×10^{-2}	128	1.05×10^{-2}	808	1.66×10^{-3}

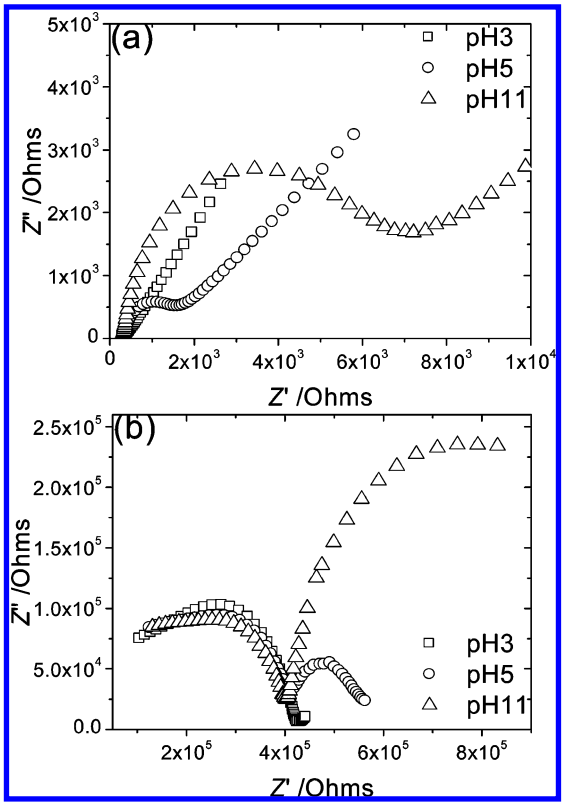

Figure 8. Nyquist plot of UA-functionalized (a) boron-doped MCD_22.8 ppm and (b) undoped MCD in 0.1 mM Fe-redox couple electrolyte of different pH: 3 (■), 5 (●), and 11 (▲).

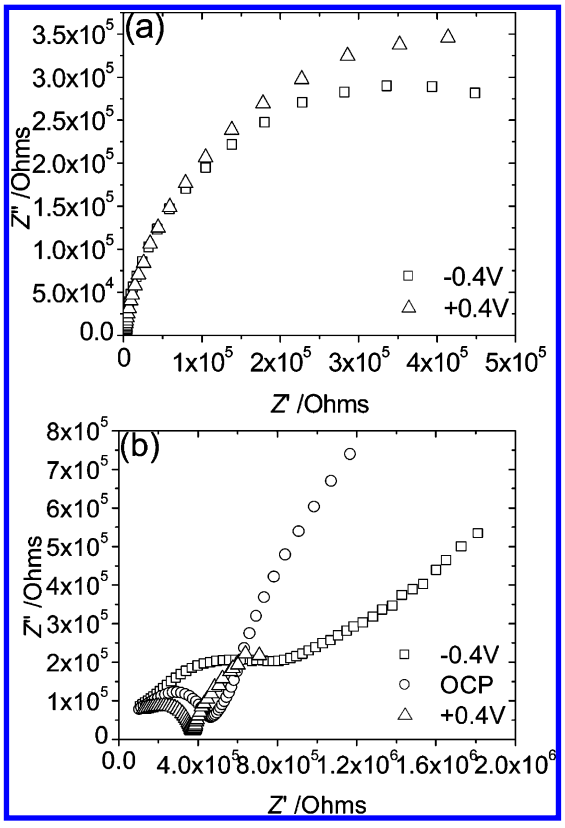

Figure 9. Nyquist plot of UA-functionalized (a) boron-doped MCD_22.8 ppm and (b) undoped MCD in PBS at −0.4 V (■), OCP (●), and +0.4 V (▲).

charge in diamond because a lightly doped diamond will have a large depletion depth arising from ionization of acceptors. Another explanation is that the electron affinity of the UA

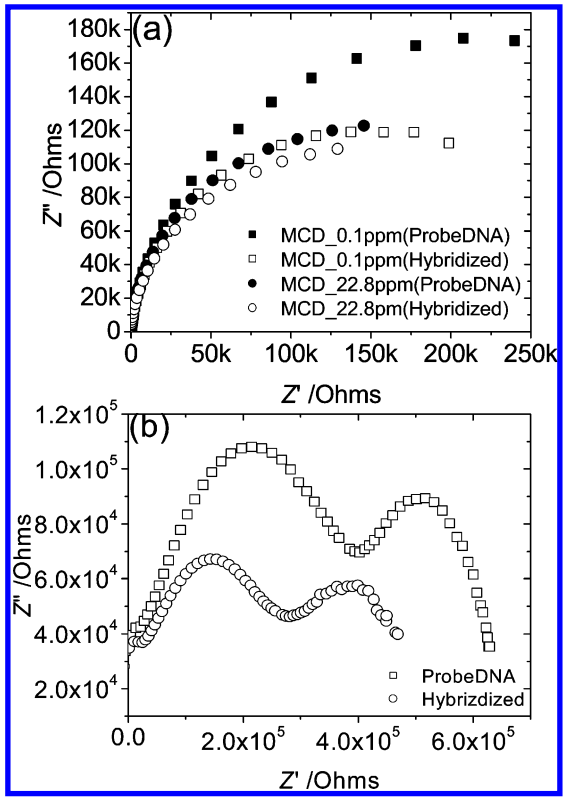

Figure 10. DNA sensing: (a) Nyquist plot of probe DNA immobilized (shaded) and after hybridization to complimentary target DNA (voided) on MCD_0.1 ppm (■) and MCD_22.8 ppm (●); (b) Nyquist plot of probe DNA immobilized on undoped MCD (■) and after hybridization to complimentary target DNA (●).

molecular layer is influenced by the pH because of protonation/deprotonation; subsequently, the different degree of charge transfer from nominally undoped diamond onto UA will affect the carrier concentration in the subsurface depletion region dramatically. The surface transfer doping model proposed by Ristein and co-workers[23] has been used to explain the reduction in surface resistance of nominally undoped diamond by several orders in magnitude when exposed to an acidic environment.

For diamond with a dopant concentration $>10^{19}$ cm^{-1}, the impedance response does not disperse with applied voltage, suggesting the pinning of the Fermi level by surface states, as shown in Figure 9a. For the nominally undoped diamond, the high-frequency loop shows a clear p-type space-charge response as a function of applied voltage as shown in Figure 9b, where the application of a negative voltage drives the p-type semiconductor to depletion,[24] as judged by the larger diameter of the high frequency loop (left-hand loop in Figure 9b) at −0.4 V compared to +0.4 V. As such, the high-frequency loop may be associated with space charge in the diamond. The observed p-type space charge response becomes weaker with the increase of dopant levels in diamond. The sensitivity of the diamond to DNA binding events is correlated with the sensitivity of its impedimetric response to pH or voltage changes. If a large change in impedance could be observed following changes in the pH of electrolyte or the voltage applied on the sample, a similarly strong response can be expected during DNA binding. This is because the binding of the DNA changed the surface charge density on the diamond, which in turn induces mirror charges in the diamond subsurface

(23) Maier, F.; Riedel, M.; Mantel, B.; Ristein, J.; Ley, L. *Phys. Rev. Lett.* **2000**, *85*, 3472.
(24) Tse, K.-Y.; Nichols, B. M.; Yang, W.; Butler, J. E.; Russell, J. N., Jr.; Hamers, R. J. *J. Phys. Chem. B* **2005**, *109*, 8523.

regions. On doped diamond with dopant concentrations $>10^{19}$ cm^{-1}, we find that there is insignificant changes in impedance following hybridization of DNA in Figure 10a; in this case, the changes in impedance occur mainly at the low frequency (<1000 Hz) and arise mainly from changes in the resistance of the molecular layer during DNA hybridization. However, on undoped diamond, following hybridization with DNA, a clear reduction in the diameter of the two loops can be seen in Figure 10b. The reduction in the diameters of the two semicircles can be explained by the reduction in charge-transfer resistance of the molecular layers following the $\pi-\pi$ stacking of the duplex DNA (low-frequency loop), as well as a reduction in the subsurface depletion due to an accumulation of holes (high-frequency loop).

4. Conclusion

We demonstrated that direct photochemical coupling with undecylenic acid (UA) is a convenient method to introduce carboxylic groups on diamond. Directly coupling with UA without headgroup protection resulted in a higher density of COOH groups than that using a protecting group involving trifluoroethyl undecenoate (TFEU). The result shows that diamond behaves differently than silicon surfaces where headgroup protection is needed to prevent attack of the silicon surfaces by acidic headgroups. Lithographically patterned DNA arrays which remained stable against repeated denaturation and rehybridization can be formed on UA-functionalized diamond. Diamond with low boron concentration ($<10^{17}$ cm^{-3}) exhibits a larger change in impedance during DNA hybridization compared to highly doped diamond, which is related to space charge effects in the former.

Acknowledgment. We thank Doreen M. Y. Lai of IMRE for providing help with the TOF-SIMS, as well as the support of NUS academic grant R-143-000-275-112.

LA063658K